

## Introduction and Motivation

- Neutron scatter cameras use the kinematics of elastic neutron-proton scattering to estimate the incoming direction of neutrons
- Neutrons must scatter twice in the scintillator volume to reconstruct incident neutron direction
- We need multiple parameters to back-project incident angle neutron cones:
  - Scintillation position along the pillar for first and second scatter
  - Proton recoil energy in first scatter
  - Time between neutron scatter events
- Evaluate best combination of scintillator, photodetector, and pillar size to estimate scintillation position, time, and brightness

## Design

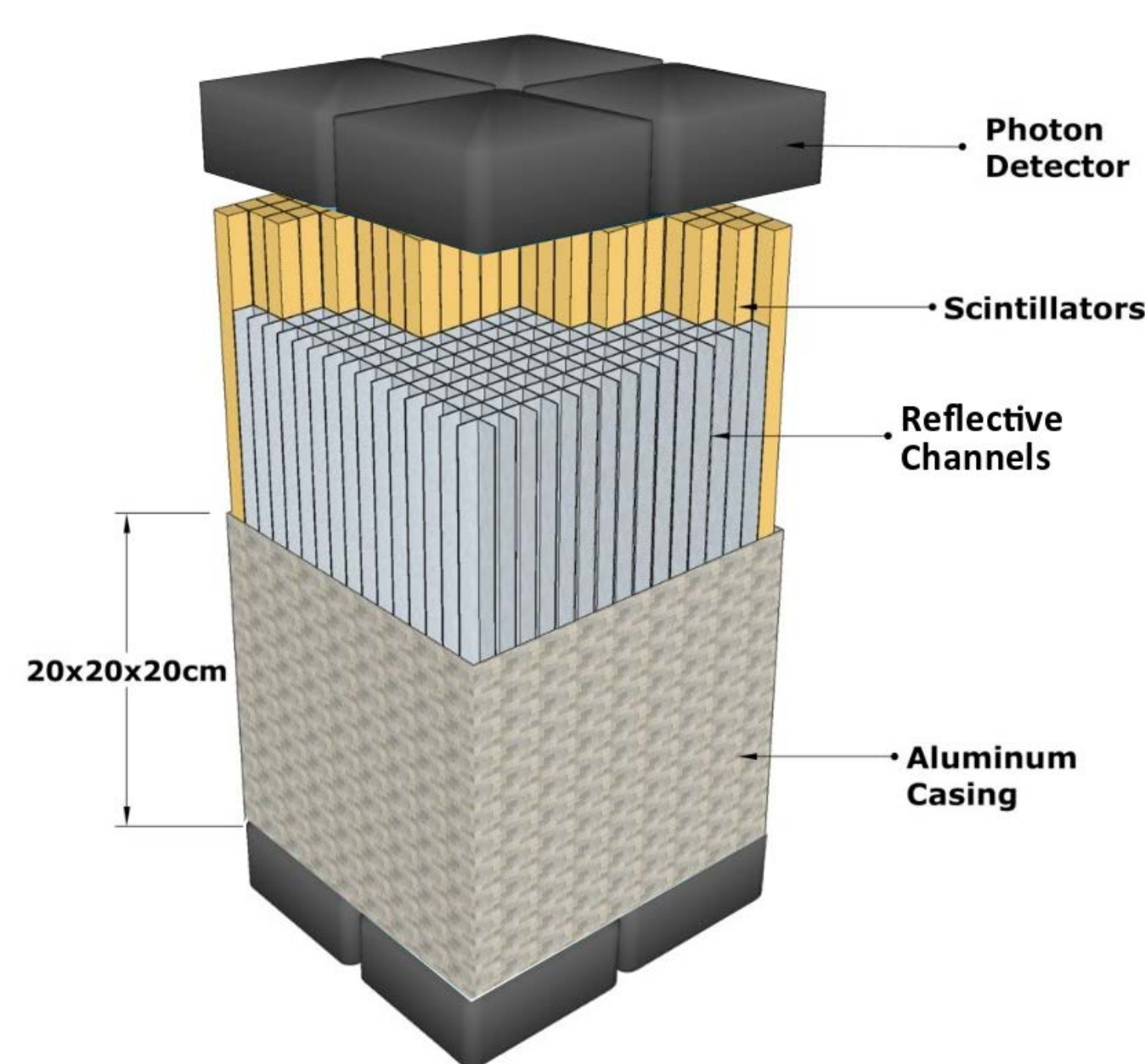


Figure 1: Instrument conceptual design using pillars of scintillator

- Instrument design uses a single, contiguous volume of organic liquid scintillator that is internally subdivided into optically isolated pillars (Figure 1)
- An air gap surrounds each scintillator pillar enabling total internal reflection
- Escaping light is reflected back into the pillar using a specular reflector lining the channel walls
- Photodetectors (PD) are affixed to opposing ends each pillar to collect scintillation light
- This design allows for an order-of-magnitude efficiency increase compared to a dual plane neutron scatter camera developed at Sandia National Laboratories

## Methods

- Position along pillar axis estimated using intensity vs. time history of charge carriers emitted by the photodetectors at each end of the pillar
- Tabulate nominal responses of scintillation photons to establish scintillation

$$R_{nom} = R_{scint}(t) * R_{chan}(t) * R_{TTS}(t) * R_{imp}(t)$$

- \* is the convolution operator
- $R_{nom}$  is the nominal response
- $R_{scint}$  is the scintillator time response
- $R_{chan}$  is the channel response
- $R_{TTS}$  is the transit time spread of the PD
- $R_{imp}$  is the impulse response of the PD

## Methods (cont.)

- Scintillation, transit time spread, and photodetector impulse responses obtained from their respective data sheets
- Channel response functions tabulated using Geant4 optical light simulation module by simulating  $10^7$  optical photons in 0.5 cm increments
- Channel response functions estimate temporal spread of photons as they propagate throughout the pillar

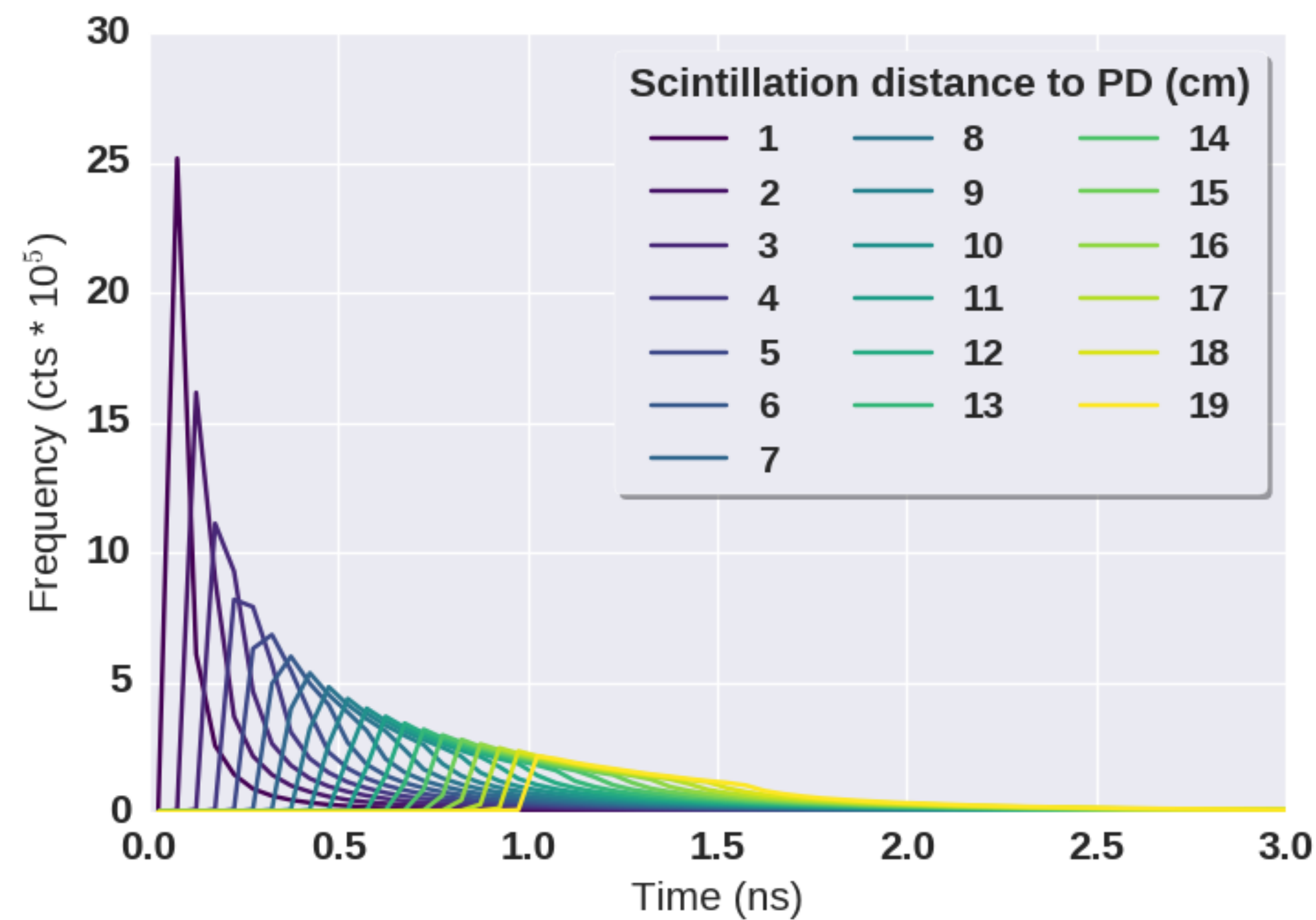


Figure 3: Channel response functions ( $R_{chan}$ ). Demonstrates temporal spread of photon arrival times at ends of pillar.

- Convolve channel response functions with scintillator response to randomly sample charge carrier arrival times in the photodetector

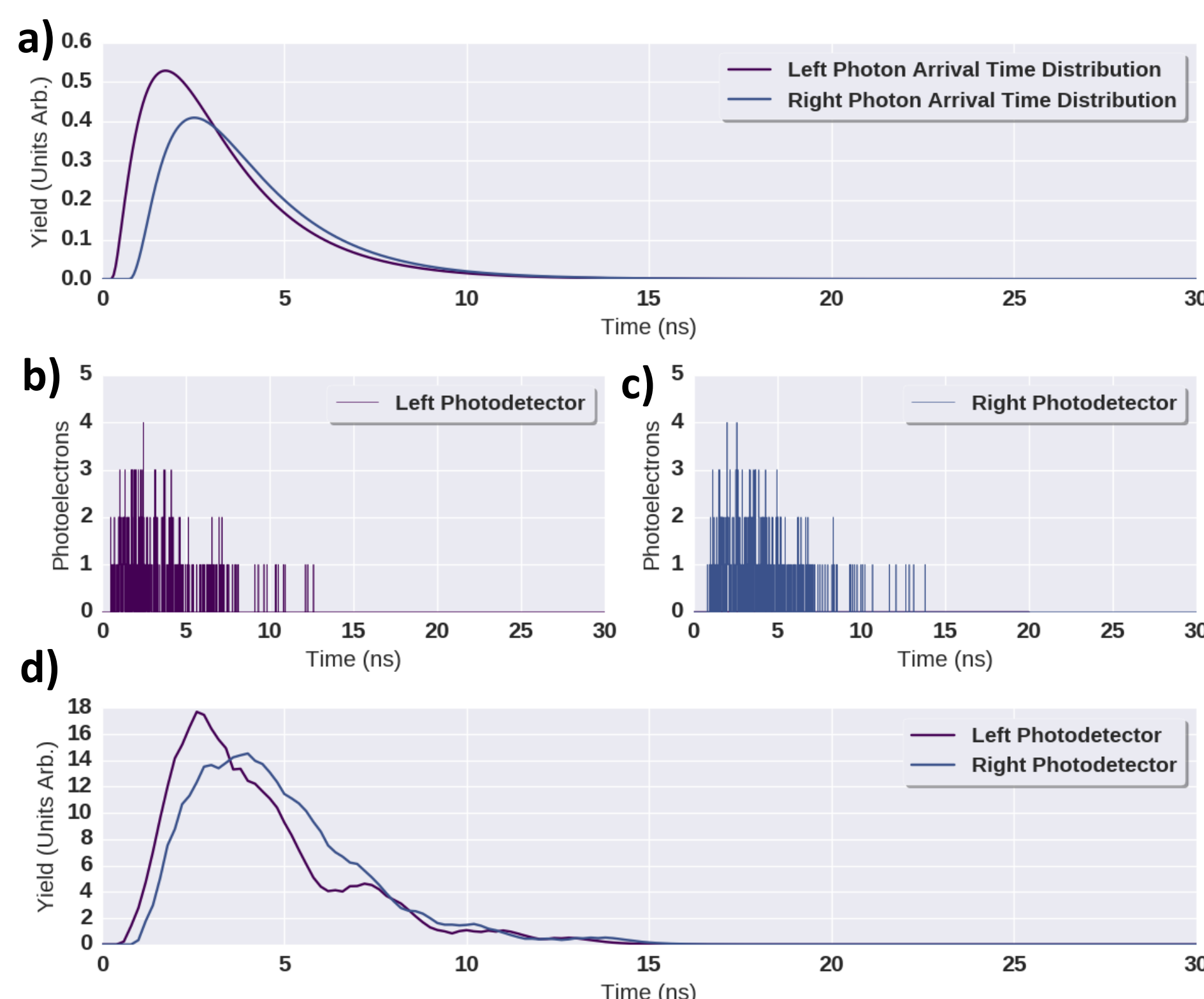


Figure 4: a) Pair of channel responses convolved with scintillator time response at true scintillation position. b,c) Randomly sampled charge carrier arrival times in photodetector using a). d) Convolve with charge carrier arrival time with transit time spread and photodetector impulse response

- We compared the observed responses (Figure 4d) to nominal responses (Figure 5) using Broyden-Fletcher-Goldfarb-Shanno minimization method and a negative log Poisson likelihood objective function

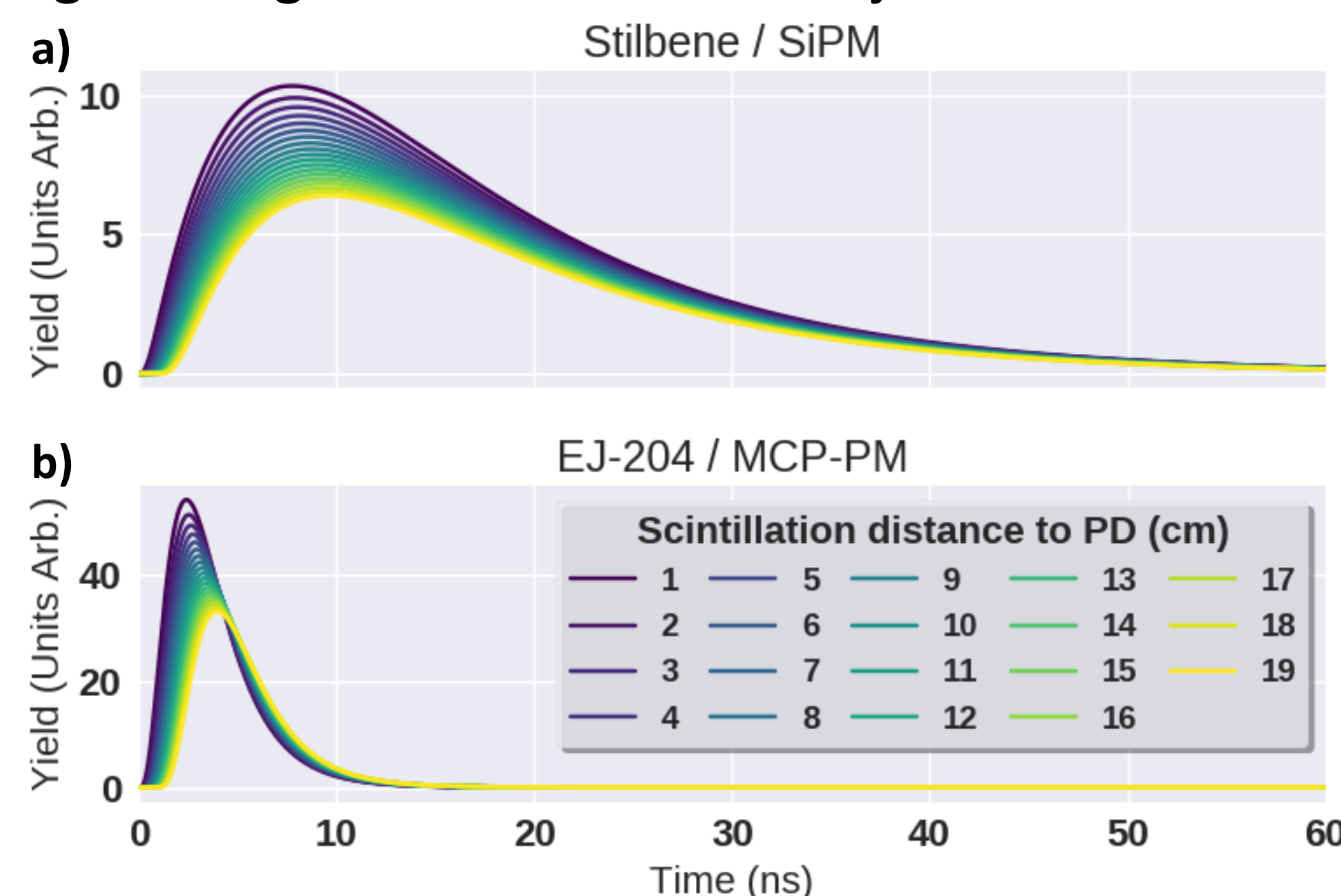


Figure 5: Nominal responses created using Equation 1. a) Responses using stilbene/SiPM combination. b) Responses using EJ-204/MCP-PM combination

## Results

- Photodetectors modeled
  - Microchannel plate photomultiplier (MCP-PM)
  - Silicon photomultiplier (SiPM)
- Scintillators modeled
  - EJ-204, EJ-232Q, stilbene
- Pillar geometry
  - 10 cm and 20 cm lengths
  - 0.5 cm and 1.0 cm side widths

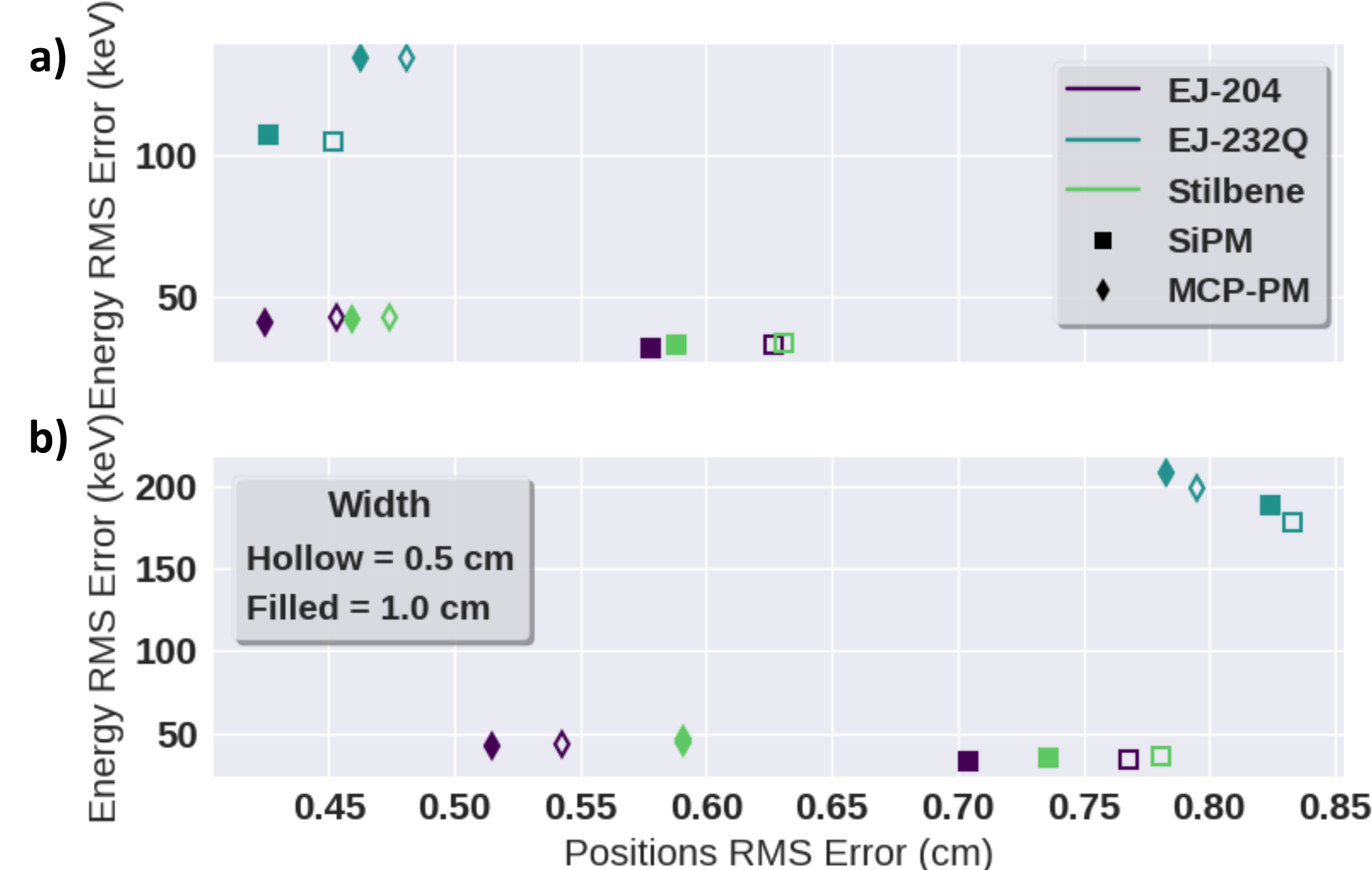


Figure 6: Scintillation position and proton recoil energy reconstruction results using a 2 MeV proton recoil. a) Results for a 10 cm pillar. b) Results for a 20 cm pillar

- Overall, best combination observed was EJ-204/MCP-PM
  - Compact charge carrier time distribution in photodetector allows for best position precision
  - Luminosity and quantum efficiency dictate proton recoil energy reconstruction precision
- Short self-attenuation length of EJ-232Q (8 cm) substantially reduces position precision for 20 cm pillar
- Proton recoil energy RMS error stays constant at 50 keV for proton recoil energies between 0.2 – 3 MeV
- Combination reconstruction ability did not change relative to each other for a 1 MeV proton recoil energy
  - A decrease in reconstruction precision observed due to reduced photostatistics

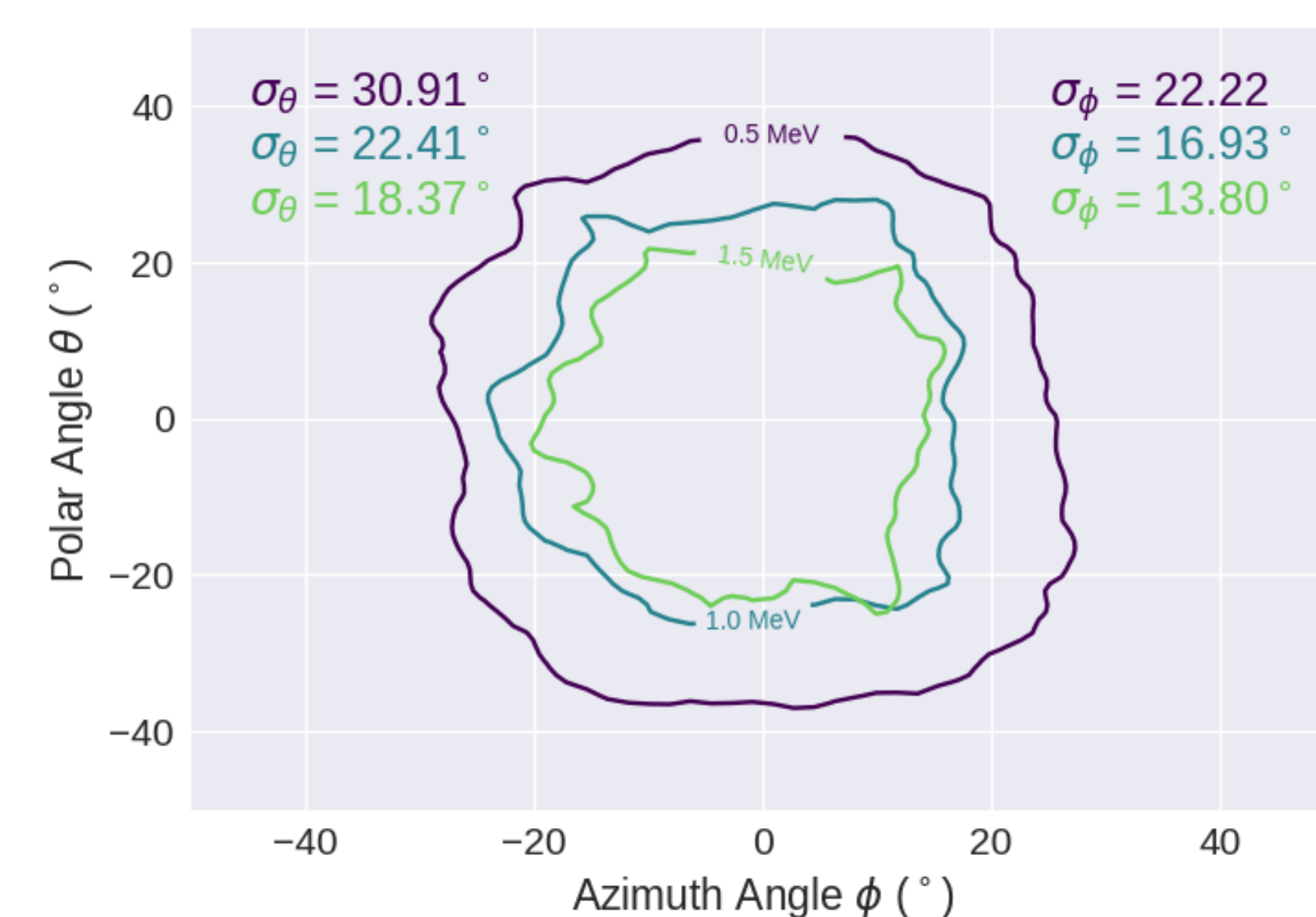


Figure 7: Detector resolution using 0.5, 1 and 1.5 MeV thresholds for neutron double scatter events. Simulated using a Cf-252 source 1 m away from center of imaging device using MCNPX-PoliMi.

- Better precision of scintillation position for higher proton recoil energies
  - Cone back-projection more accurate
- Discriminate on double scatter events where both interactions have proton recoil energy estimates above threshold
- Improved back-projected image resolution for higher energy thresholds
  - At the cost of fewer double scatter events passing threshold criteria